Experimental and numerical second order diffracted waves around an array of 4 cylinders.

Scolan Y.-M., ESIM, Marseille, France
Malenica Š, BUREAU VERITAS, La Défense, France

1. Introduction

The diffraction of regular waves around an array of 4 vertical cylinders is investigated. Results from existing theoretical models are compared with experimental data acquired in the frame of a french CLAROM project started in 1996. Encouraging results are obtained for both first and second order quantities in the limit of small wave steepness.

Another aspect is also emphasized concerning the existence of high localised second order wave elevations in the spacing between the two front columns. The computations show that second order maxima is only due to diffraction and they occur precisely where the first order envelop vanishes. The existence of trapped modes may explain these resonant like phenomena.

In the following developments, the experimental set-up is first described, then the two different numerical approaches are outlined. Some significant results of comparison are finally shown.

2. The experimental set-up

The set-up (described below) is simply composed of bottom mounted vertical cylinders of circular cross section. One of the longitudinal walls of the basin is used as a symmetry plane; the TLP model is thus composed of 2 cylinders at incidence 0°. With this choice the problems of blockage are practically avoided and it significantly reduces the perturbation due to the reflected waves on the opposite longitudinal wall. An additional wave absorber is placed on this wall. These precautions are necessary to obtain a sufficiently long period for data acquisition without spurious harmonics. This is of crucial importance particularly when second order quantities are to be measured. Seven wave gauges are placed in the vicinity of the four columns as described below.

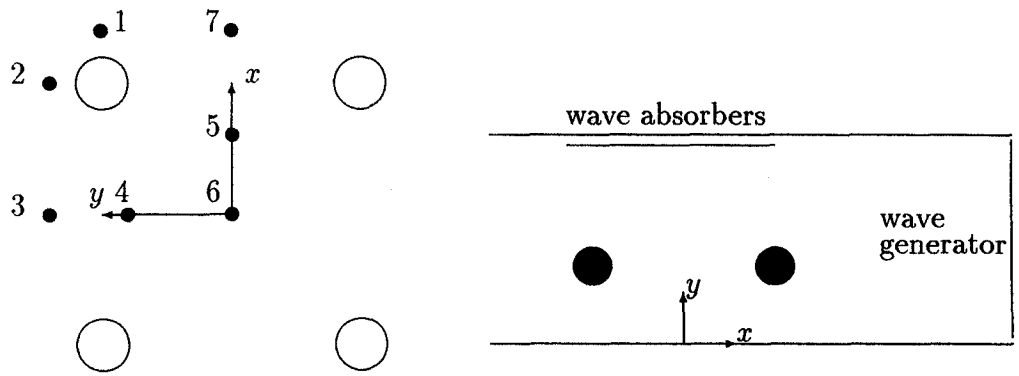

3. The numerical tools

The second order diffraction problem can be formulated for the corresponding potentiel $\phi_D^{(2)}$ as follows:

$$P_D^{(2)}\begin{cases} \Delta\phi_D^{(2)} = 0 & \text{in the fluid domain} \\ \phi_{D,z}^{(2)} - \frac{4\omega^2}{g}\phi_D^{(2)} = \alpha^{id} + \alpha^{dd} & \text{on the free surface } z = 0 \\ \phi_{D,r}^{(2)} = -\phi_{I,r}^{(2)} & \text{on the cylinders} \\ \phi_{D,z}^{(2)} = 0 & \text{on the sea-bottom } z = -h \\ Rad\left(\phi_D^{(2)}\right) & \text{in the far field} \end{cases} \quad (1)$$

The 2^{nd} order incident potential $\phi_I^{(2)}$ is known analytically. The right hand side of the free surface condition exhibits in the far field two wave interactions; here α^{id} and α^{dd} correspond to the interactions incident/diffracted and diffracted/diffracted respectively. The radiation condition usually follows from an analysis of the far field wave decomposition into free and locked components.

To solve this BVP, two different numerical approaches are used: semi-analytical formulations and numerical diffraction programs developed in the frame of potential flow theory. Both

approaches use **semi-analytical first order solutions** to account for the interaction of cylinders. The formulation by McIver & Evans (1984) is approximate and the other one by Linton & Evans (1990) is exact. Discrepancies exist and some of them are exposed here and in Scolan *et al.* (1997).

The second order **semi-analytical approach** uses the Linton & Evans' first order solution. It is based on the decomposition of the second order potential into several potentials, each verifying a particular Boundary Value Problem (BVP) solved semi-analytically. This is presented in Malenica (1997).

The other approach is a **full numerical solution of the BVP** expressed above by using an integral equation and the Rankine Green function (see Scolan 1989). The main aspect concerns the radiation condition which is based on the decomposition of the far field into locked and free waves (see Molin 1979).

4. Some results

Figures (1) compare the numerical or experimental total second order quantities. Those include the incident and diffracted components (noted $\eta_I^{(2)}$ and $\eta_D^{(2)}$ respectively) and the quadratic contributions (noted $\eta_{Q(1)}^{(2)}$) coming from first order.

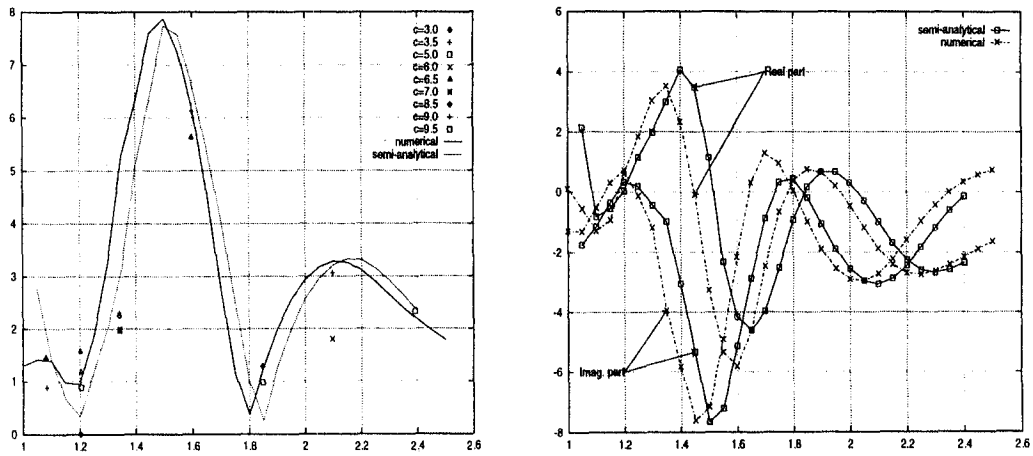

Figure 1: *(left)* modulus of the 2^{nd} order wave elevation vs period (sec) at gauge $N°5$, radius 0.280 and spacing 1.334; experimental data are marked for different wave steepnesses; *(right)* numerical and semi-analytical real and imaginary parts of $\eta^{(2)}$.

The plotted quantities are non dimensioned with kA^2 where k and A are the wave number and the incident wave amplitude respectively. The highest second order elevations $\eta^{(2)}/kA^2 \approx 8$ occur at the gauge $N°5$ ($x/d = 0.39$) and at about $T = 1.5s$. The shift of period illustrates the differences between the two first order formulation. The overall trend is however very similar.

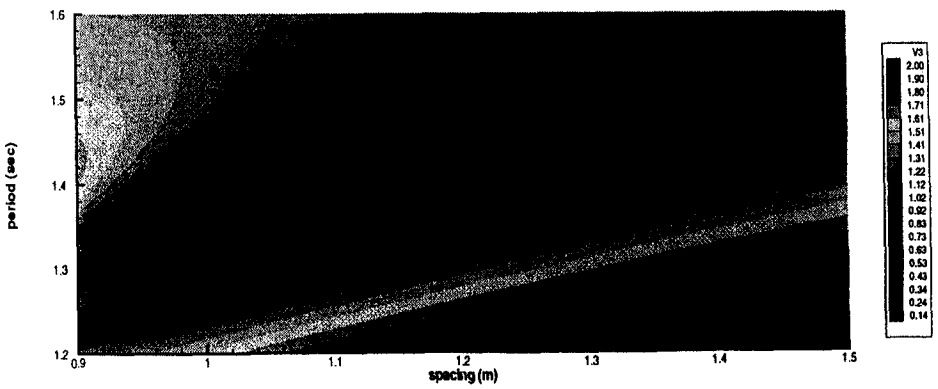

Figure 2: locations of $\eta^{(1)}$ modulus minima at mid-point between the two front cylinders.

A study of the second order wave pattern shows that localised high elevations occur between the two front cylinders. This could suggest resonant like phenomena somewhere between the cylinders. A more precise study shows that first order wave elevations vanish in the same area. Hence a parametric study should first provide couples of spacing and wave period for which there exist areas where first order elevations vanish. Such locations are determined along the symmetry axis ($y = 0$) and between either upstream or downstream cylinders. For example figure (2) shows the locations in the plane ($spacing, period$) of the $\eta^{(1)}$ modulus minima calculated exactly at the mid-point between the two front cylinders. Computations are thus performed for different couples ranging along a line which joins the 2 points $(1.0, 1.348)$ and $(1.25, 1.48)$. As a matter of fact, the obtained results (not reproduced here) show the same characteristics. To illustrate this the total second order wave pattern is plotted in figure (3) for the data $d = 100$ and $T = 13.48$ with the radius $a = 28$ (corresponding to a geometry 100 times larger than the model one). A spot of high elevation is clearly noticeable exactly between the two upstream cylinders. A question arises whether this is due to forcing term of the free surface condition or this is due to pure diffraction. For that in the left figure, the 1^{st} order elevation is compared to the different 2^{nd} order quantities. One may note that:

- the second order diffraction is clearly the dominant contribution,
- this component reaches its maximum precisely where the total 1^{st} order elevation vanishes,
- the 2^{nd} order diffraction is the only explanation for this local effect since the quadratic terms bring almost negligible contribution even if it is thought that $\vec{\nabla}^2\phi^{(1)}$ should contribute significantly,
- the 1^{st} order elevation, the right hand side $(\alpha^{id} + \alpha^{dd})$ and the mean value have a very similar variation along the axis,
- the forcing term of the free surface condition seems not important enough to explain this phenomenon.

Another couple is then computed for a different location of vanishing first order elevation; the listed conclusions above seem confirmed as shown in figures (4). Here one should note that the forcing term of the free surface condition decreases significantly at the location of interest.

From the first studied data (see figure 3) one can compute the positions of the near-trapped modes (if existing) associated to this configuration. This is done by calculating the force acting on each cylinder. This force (F) is usually made non dimensioned with the force (F_s) acting on a single cylinder in isolation as it is done in Evans and Porter (1997). From our computations a very sharp peak of force ($F/F_s \approx 12$) is observed at $ka \approx 0.7957$ corresponding here to $T \approx 11.9s$ and for a spacing $d/a = 2.5$ (made non dimensioned with the cylinder radius). This result must be considered with precaution as the approximated first order solution is used.

However, as the spacing increases the peak of force is shifted towards higher periods. For the present spacing $d/a \approx 3.57$, a peak of the force ($F/F_s \approx 1.6$) is at about $T \approx 13.7s$. This is close to the first order incident wave but far from the period of the corresponding second order free wave system. A parametric study by varying both the spacing and the period should bring some more elements of answer. Those will be presented at the workshop.

Acknowledgements: This work is done in a CLAROM Joint Industry Project. The authors thank the partners: Principia RD (leader), Total, Bouygues Offshore, Doris Eng., Bureau Veritas, Ifremer and Sirehna to allow the publication of the present results.

6. References

- Evans D.V. & Porter R., 1997, "Near-trapping of waves by circular arrays of vertical cylinders.", Applied Ocean Research, Vol.19, pp 83–99.
- Malenica Š, 1997b, "Second order interaction of water waves with arrays of vertical circular cylinders", Proceedings of the 2nd Congress of Croatian Society of Mechanics, pp. 599-606, Supetar, Croatia.
- Linton C.M. & Evans D.V., 1990, "The interaction of waves with arrays of vertical circular cylinder in a channel.", J. Fluid Mech., Vol 215, pp 549–569.
- Mc Iver P. & Evans, D.V., 1984, "Approximation of wave forces on cylinder arrays", Applied Ocean Research, Vol.6, $N°2$, pp 101–107.
- Molin B., 1979, "Second-order diffraction loads upon three-dimensional bodies", Applied Ocean Research, Vol. 1, $N°4$.
- Scolan Y.-M., 1989, "Contribution à l'Etude des Non-Linéarités de Surface Libre. Deux cas d'application...", PhD Thesis, University Paris 6.
- Scolan Y.-M., Malenica Š & Martigny D., 1997, "Experimental and numerical studies of the TLP's airgap.", to be presented at ISOPE Conf., Montreal, Canada.

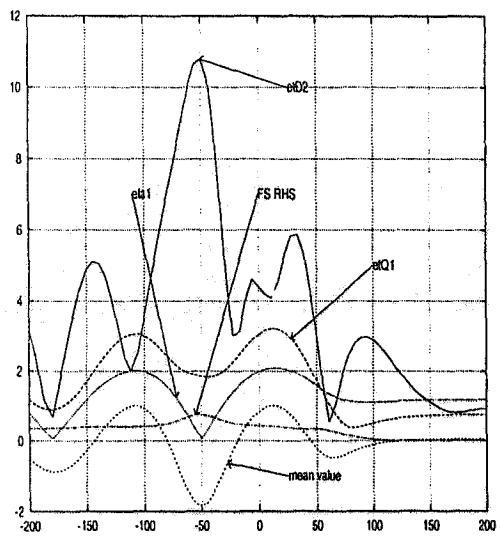

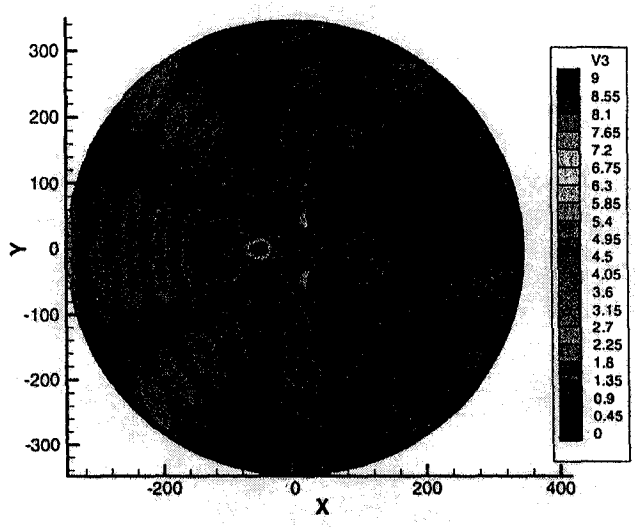

Figures 3: variation of the contributions to the free surface elevation $|\eta_I^{(2)}|$, $|\eta_D^{(2)}|$, $|\eta_{Q(1)}^{(2)}|$, mean value, $|\eta^{(1)}|$, right hand side of the free surface condition $\alpha^{id} + \alpha^{dd}$; gap/radius= 100/28 and $T = 13.48s$

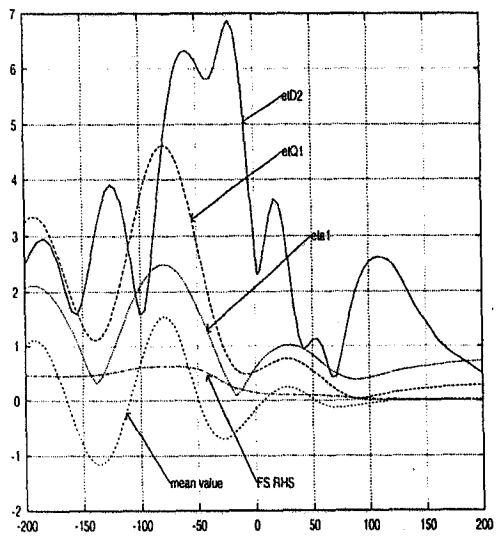

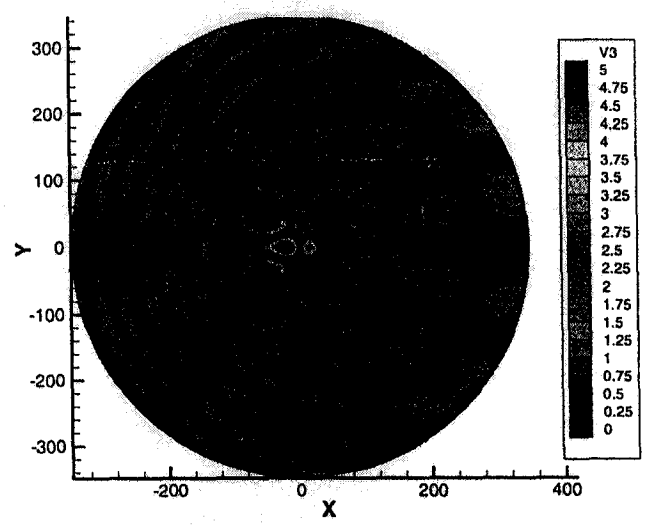

Figure 4: see caption above; gap/radius= 106/28 and $T = 11.8s$